CRITICAL POINTS IN FLOW PATTERNS

A. E. Perry and B. D. Fairlie[1]

Department of Mechanical Engineering
University of Melbourne, Melbourne, Australia

1. Introduction

The "phase-plane" and "phase-space" methods of exploring the properties of solutions of ordinary differential equations have proved to be extremely successful in the field of nonlinear dynamical systems. The methods do not yield a complete solution; but by locating certain critical points, linearizing about them, and exploring other topological features of the solution trajectories, the most important features of the solution of a given differential-equation set can be displayed in a descriptive manner.

Following a suggestion of Kronauer (1967) the authors have applied these techniques to fluid flow problems. Oswatitsch (1958) and Lighthill (1963) examined viscous flow patterns close to a rigid boundary and classified certain critical points which can occur. The mathematics used was equivalent to the phase-plane trajectory analysis mentioned above. However, analysing such critical points in the framework of phase-space trajectory analysis gives the study a unified approach and enables a wealth of topological language to be utilized which seems in some instances to be less ambiguous than the terms used in fluid mechanics, such as separation points, separation lines, regions of reversed flow, and so on.

Here the authors apply this technique to the problem of viscous flow and then extend the approach to inviscid rotational flow, with slip at the boundary. This appears to be the appropriate model for turbulent boundary layers approaching obstacles. The various types of critical points are classified for this inviscid type flow.

Although the positions of the critical points cannot always be predicted analytically, the authors feel that the study which follows will aid the experimenter in knowing what to look for in wind-tunnel flow-pattern studies and help him to identify the types of singular points which occur. This would aid him greatly in sketching flow patterns and in gaining an understanding of them. The experienced investigator will quite often be able to guess the sort of critical points that are likely to occur in a proposed situation and hence he

[1] *Present address*: Aeronautical Research Laboratories, Melbourne, Victoria, Australia.

will know fairly well the overall flow pattern which would result. There are certain topological restraints that greatly restrict the range of possible flow patterns for a given geometry. For further information regarding this and for more detailed studies of phase-space techniques, the reader is referred to Kaplan (1958), Pontryagin (1962), and Andronov *et al.* (1966).

2. Classification of Critical Points

Any set of ordinary differential equations which are autonomous may be written without loss of generality as a set of coupled first-order equations thus

$$\dot{\mathbf{x}} = H(\mathbf{x})$$

As time proceeds, the solutions of such a set trace out trajectories in the phase space $\mathbf{x}$, and each trajectory is completely defined by initial conditions $\mathbf{x}_0$. If the equations are autonomous, i.e., if time does not appear explicitly, then trajectories will in general not cross and so all solutions and trajectory slopes $\dot{x}_1/\dot{x}_2 = dx_1/dx_2$, etc., are unique. However, there may exist certain critical points in the phase space where the slopes are indeterminate, i.e., $\dot{x}_1/\dot{x}_2 = 0/0$ and at such points, it is often the case that trajectories do cross.

For simplicity, consider the cases where the solution trajectories are confined to one plane, i.e.,

$$\dot{x}_1 = P(x_1, x_2), \qquad \dot{x}_2 = Q(x_1, x_2)$$

In general P and Q will be nonlinear functions. It is assumed in what follows that in the region of a critical point, the equations are linearizable and may be expressed as

$$\begin{bmatrix} \dot{x}_1 \\ \dot{x}_2 \end{bmatrix} = \begin{bmatrix} a & b \\ c & d \end{bmatrix} \begin{bmatrix} x_1 \\ x_2 \end{bmatrix}$$

that is,

$$\dot{\mathbf{x}} = F \cdot \mathbf{x}$$

This is equivalent to the assumption that the equations are Taylor series expandable in the region of the critical point and that terms of order higher than one may be safely ignored. The matrix F (the Jacobian) will have eigenvalues λ_1 and λ_2 which may in general be real or complex. The corresponding eigenvector slopes are

$$m_1 = (\lambda_1 - a)/b = c/(\lambda_1 - d)$$

and

$$m_2 = (\lambda_2 - a)/b = c/(\lambda_2 - d) \tag{1}$$

which for the case of λ_1 and λ_2 real, may be shown to correspond to the slopes of certain special trajectories which emanate from the critical point.

By the use of a suitable affine transformation (i.e., rotation of axes x_1 and x_2 and linear stretching of these coordinates) the trajectories can be described in a "canonical" form in terms of these new transformed coordinates. Such a transformation (see Fig. 1a) can always be found which will reduce all trajectories to either simple power laws or logarithmic spirals, depending on whether λ_1 and λ_2 are real or complex, respectively.

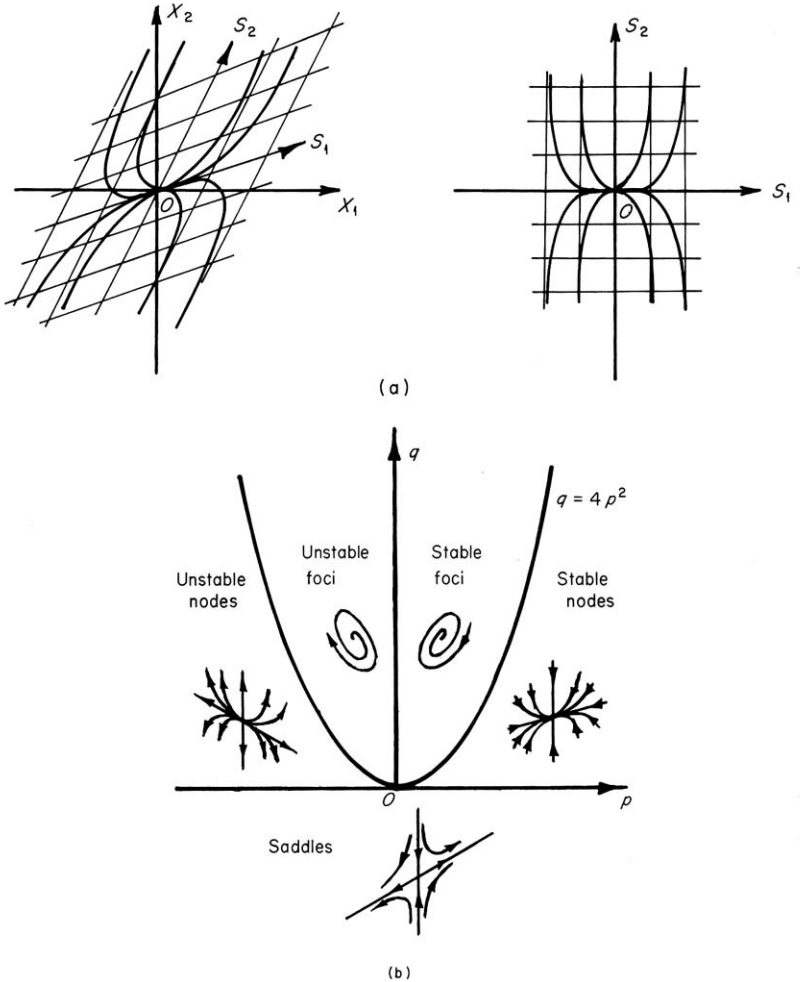

FIG. 1. Classification and transformation of critical points. (a) Demonstration of an affine transformation from x_1x_2 plane to s_1s_2 plane. (b) p-q chart which shows classification of critical points.

The classification of possible critical points may be represented as shown in Fig. 1b where

$$(2) \qquad p = -(a + d) = -\operatorname{tr} F, \qquad q = (ad - bc) = \begin{vmatrix} a & b \\ c & d \end{vmatrix} = \det F$$

and

$$\lambda_{1,2} = -\tfrac{1}{2}[p \mp (p^2 - 4q)^{1/2}]$$

Critical points corresponding to values of p and q along the axes ($p = 0$ or $q = 0$) and on the parabola $p^2 = 4q$ are degenerate forms.

The classification of critical points in phase-planes may be extended to cases where a three- or higher-dimensional phase space is required, but this involves considerable complexity. Three-dimensional phase space will be considered here, but attention will be confined to planes that contain trajectories (when they exist) allowing the simple phase-plane techniques to be applied.

3. Application to Flow Patterns

Consider the flow over a surface (defined by the xy plane) of a real viscous fluid. It is assumed that the velocity components are Taylor series expandable about some critical point, thus

$$(3) \qquad \mathbf{U} = \phi(\mathbf{X})F\mathbf{X}$$

where $\phi(\mathbf{X})$ is a scalar function of real physical space $\mathbf{X}$, F is a 3×3 Jacobian matrix, and $\mathbf{U}$ is the velocity vector. See Fig. 2.

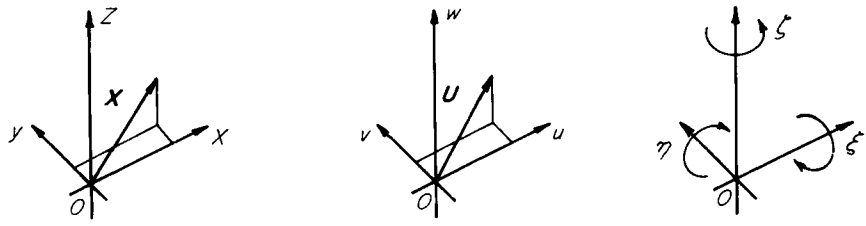

Fig. 2. Notation used.

Let t = real time and define a new time variable τ such that

$$(4) \qquad d\tau = \phi(\mathbf{X})\, dt$$

Equation (3) can be put into phase-space form thus

$$(5) \qquad \mathbf{X}' = F\mathbf{X}$$

where the prime denotes a differentiation with respect to τ. In expanded form this is

$$\begin{aligned} x' &= a_1 x + b_1 y + c_1 z \\ y' &= a_2 x + b_2 y + c_2 z \\ z' &= a_3 x + b_3 y + c_3 z \end{aligned} \tag{6}$$

Hence, the assumption that the velocity components are Taylor series expandable about a critical point is equivalent to assuming that the (autonomous) partial differential equations for fluid flow can be reduced to a set of ordinary autonomous differential equations which have a critical point in a phase-space which corresponds to physical space.

For viscous flow, the no-slip condition requires that $\mathbf{U} = \mathbf{0}$ at $z = 0$ for all x and y and hence $\phi(\mathbf{X})$ in Eq. (3) becomes

$$\phi(\mathbf{X}) = z \qquad \text{and} \qquad d\tau = z\, dt$$

The description of a flow pattern via Eq. (6) is best illustrated by an example. Consider the case of a three-dimensional laminar boundary layer. This would be expressed as

$$\begin{aligned} u &= z(a_1 x + b_1 y + c_1 z) \\ v &= z(a_2 x + b_2 y + c_2 z) \\ w &= z(a_3 x + b_3 y + c_3 z) \end{aligned} \tag{7}$$

These expressions are substituted into the Navier–Stokes equations and the continuity equation with only the first-order terms retained. This results in relationships between the coefficients a_1, b_1, c_1, etc. As far as possible, the coefficients are expressed in terms of "measurable" quantities such as the surface pressure and surface vorticity and their various xy plane derivatives. For the latter quantities use must be made of the definition of vorticity and Fig. 2 shows the notation used.

Equations (6) reduce to

$$\begin{aligned} x' &= \eta_x x + \eta_y y + (P_x/2\nu)z \\ y' &= -\xi_x x - \xi_y y + (P_y/2\nu)z \\ z' &= \tfrac{1}{2}(\xi_y - \eta_x)z \end{aligned} \tag{8}$$

P and ν are the kinematic pressure and viscosity respectively and the subscript denotes partial differentiation. All coefficients in (8) are evaluated at the critical point. For simplicity, consider the case of a flow with a plane of symmetry in the xz plane so that

$$\xi_x = \eta_y = P_y = 0$$

This could represent a symmetrical flow in a diverging duct in which secondary flows give rise to cross-stream gradients of longitudinal vorticity (ξ_y) at the surface. The critical points occurring in any plane containing trajectories may now be examined.

For the surface ($z = 0$) Eqs. (8) give

$$\begin{bmatrix} x' \\ y' \end{bmatrix} = \begin{bmatrix} \eta_x & 0 \\ 0 & -\xi_y \end{bmatrix} \begin{bmatrix} x \\ y \end{bmatrix} \tag{9}$$

Hence from (2), $p = -(\eta_x - \xi_y)$ and $q = -\eta_x \xi_y$.

The type of critical point occurring in the surface thus depends on the relative magnitudes of ξ_y and η_x. Consider the case when both are negative. In this case q is negative and from Fig. 1 the critical point is a saddle. The general shape of the trajectories in the vicinity of the critical point is shown in Fig. 3 for various cases.

In the plane of symmetry ($y = 0$), Eqs. (8) become

$$\begin{bmatrix} x' \\ z' \end{bmatrix} = \begin{bmatrix} \eta_x & P_x/2v \\ 0 & \frac{1}{2}(\xi_y - \eta_x) \end{bmatrix} \begin{bmatrix} x \\ z \end{bmatrix} \tag{10}$$

Hence $p = -\frac{1}{2}(\eta_x + \xi_y)$ and $q = \frac{1}{2}\eta_x(\xi_y - \eta_x)$.

The type of critical point may be determined from the p-q chart as shown in Fig. 4 for both η_x and ξ_y again negative. For $\eta_x/\xi_y > 1$, q is negative, and the critical point is a saddle [case (a) Fig. 4]. For $\eta_x/\xi_y < 1$, the critical point becomes a node [case (c)]. For $\eta_x/\xi_y = 1$, the critical point becomes a degenerate form [case (b)]. Case (c) illustrates the ambiguity in terminology used in fluid mechanics. Although "reversed" flow is involved, the "separation" point could also be thought of as a point of reattachment. In nonlinear dynamics, this critical point is unambiguously described as a "stable node."

For case (a) above, it may be shown that the special trajectories labelled s_1 and s_2 have slopes m_1 and m_2 given by Eq. (1). Any trajectory such as these which emanate from a critical point is known as a sepratrix. The same applies to Fig. 3 where the terminology "separation lines" is often used to describe those sepratrices toward which neighbouring trajectories rapidly asymptote.

It should also be noted that in Fig. 3 it can be shown that $m_1 = \infty$ and $m_2 = 0$ which is a canonical form. Returning to Fig. 4, if $m_1 = \tan\theta$, then

$$\tan\theta = 2v(\tfrac{1}{2}\xi_y - \tfrac{3}{2}\eta_x)/P_x \tag{11}$$

Lines along which trajectory slopes are constant are called isoclines. A knowledge of these isoclines further aids the sketching of the trajectories. All rays emanating from critical points are isoclines. Examples are shown in Fig. 4.

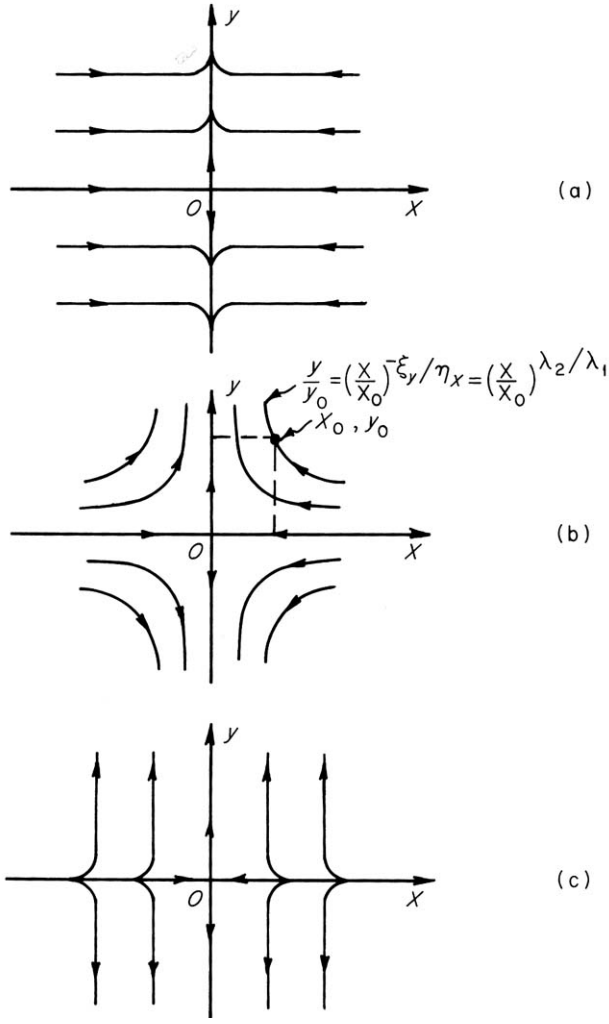

FIG. 3. Various cases of surface trajectories for symmetrical three-dimensional laminar separation. (a) $\eta_x/\xi_y \gg 1$; (b) $\eta_x/\xi_y \simeq 1$; (c) $\eta_x/\xi_y \ll 1$.

By allowing $\xi_y \to 0$, one obtains θ for the two-dimensional case as

$$\tan \theta = -3\nu\eta_x/P_x \tag{12}$$

which corresponds to the classical two-dimensional laminar-separation angle as derived by Lighthill (1963) and others. In the surface plane, allowing $\xi_y \to 0$ yields the degenerate case of a line of critical points ($q = 0$) again corresponding to the classical two-dimensional separation.

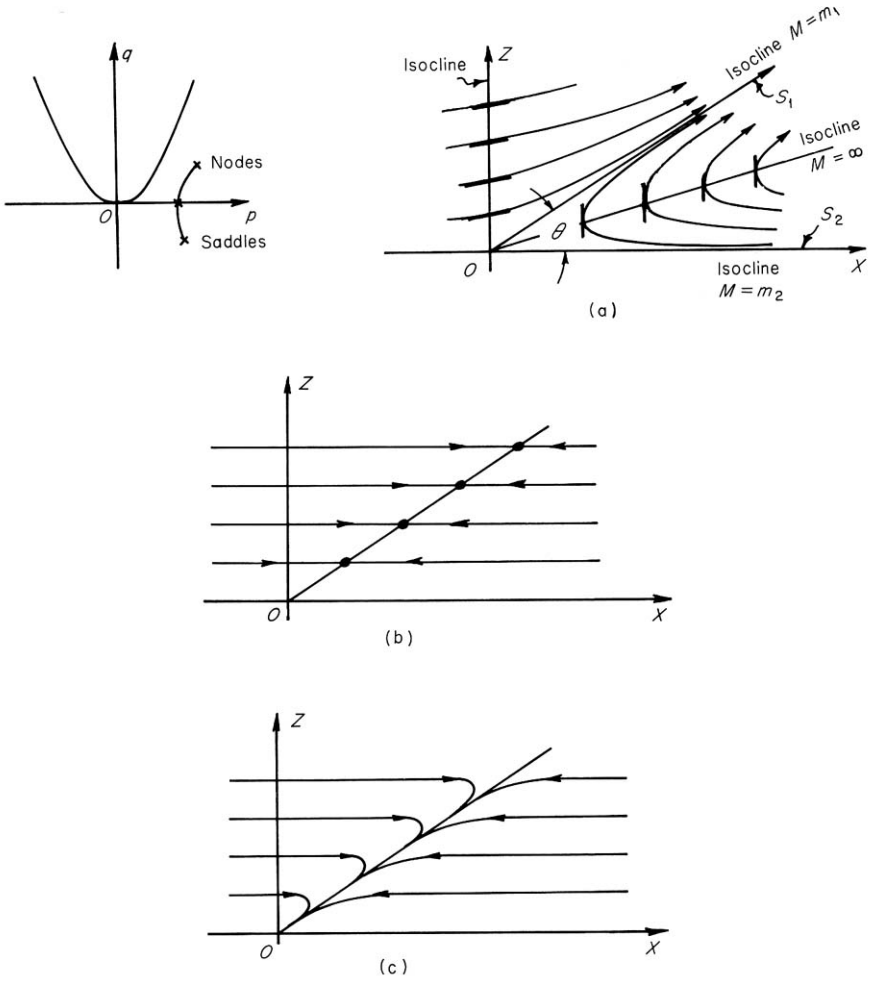

FIG. 4. Various cases of symmetrical three-dimensional laminar flow separation with p-q chart for symmetrical laminar-flow separation. Trace shown on p-q chart corresponds to a variation in η_x/ξ_y; (a) x-z plane trajectories for $\eta_x/\xi_y \gg 1$; (b) for $\eta_x/\xi_y = 1$; (c) for $\frac{1}{3} < \eta_x/\xi_y < 1$.

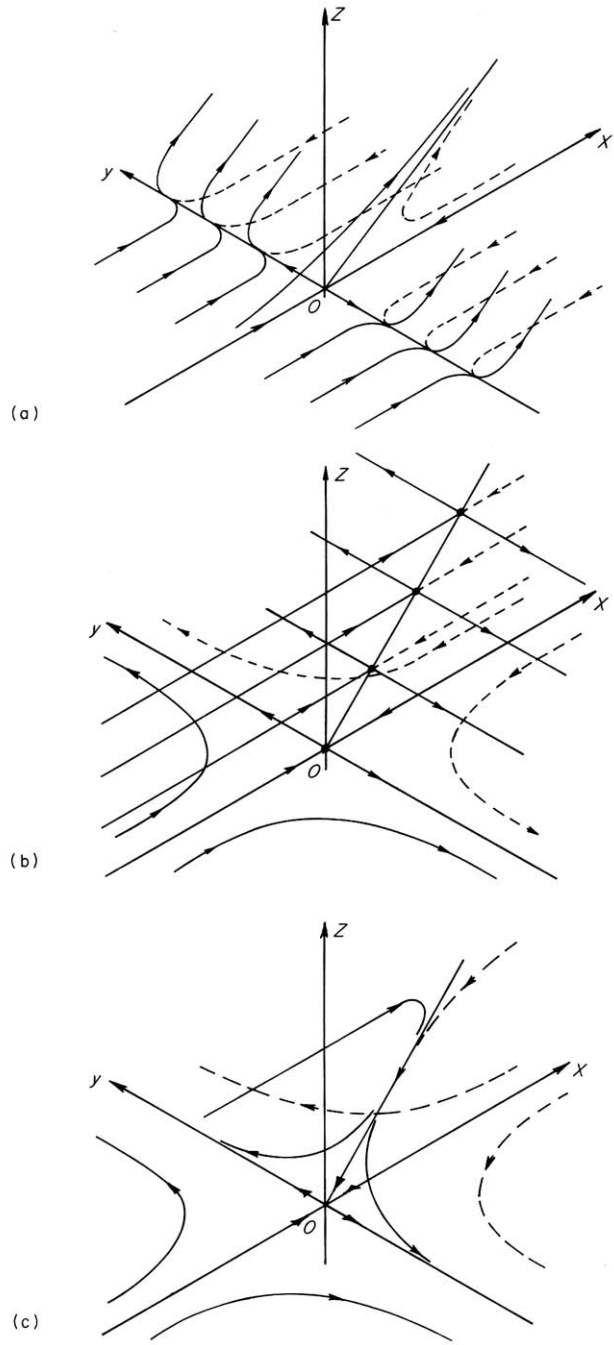

FIG. 5. Oblique view (isometric projection) of symmetrical, three-dimensional laminar flow separation. (a) $\eta_x/\xi_y \gg 1$; (b) $\eta_x/\xi_y = 1$; (c) $\frac{1}{3} < \eta_x/\xi_y < 1$.

So far two planes containing trajectories have been considered. Another plane that contains a set of trajectories is defined by the trajectory s_1 and the y axis. This is often called the "separation surface." In this plane, inclined at an angle θ to the xy plane, the appropriate type of critical point may also be determined by using coordinates s_1 and y. For case (a) a node results, case (b) is degenerate, and in case (c) a saddle is produced. Figure 5 shows some composite diagrams. These viscous flow results were also studied by Oswatitsch (1958).

4. Inviscid, Constant Vorticity Flows

It has been found by several authors that for an adverse-pressure-gradient two-dimensional turbulent boundary layer in the vicinity of a separation point, the major characteristics of the flow may be adequately represented by a layer of constant vorticity with slip at the boundary. For example, Smith (1970) considered such a representation for the flow in the region of the trailing edge of an aerofoil. The present authors (e.g., see Fairlie, 1973) considered such a model in relation to two-dimensional separation bubbles. They found that the model provided good agreement with experiment.

For a constant vorticity layer with slip at the boundary, ϕ is a constant and for $w = 0$ at $z = 0$ for all x and y, the equations become

$$\begin{aligned} u &= \dot{x} = a_1 x + b_1 y + c_1 z \\ v &= \dot{y} = a_2 x + b_2 y + c_2 z \\ w &= \dot{z} = c_3 z \end{aligned} \tag{13}$$

where the dot denotes differentiation with respect to real time.

Again, substitution into Navier–Stokes and continuity equations yields a series of quadratic and linear equations relating the coefficients to surface pressure and vorticity derivatives. It is of interest that for this case, the viscous terms in the Navier–Stokes equations are zero and that the first derivatives of surface pressure P_x, P_y, and P_z at a critical point are all zero. Since the coefficient equations contain quadratic terms, the analysis may take various alternative routes.

It is found that all critical points are degenerate and the various possibilities are shown on the p-q chart in Fig. 6a. The corresponding trajectories are also shown in Fig. 6 together with the resulting restrictions on pressure derivatives and vorticity components. If the xz plane is a plane of symmetry, then for $P_{xx} < 0$ (i.e., a pressure maximum), the critical point is a saddle.

In this case, if u, v, and w are linearizable as in Eq. (13), then only η can exist and so close to the critical point two-dimensional flow occurs.

The separation or reattachment angle θ is then given by

$$\tan\theta = \pm 2(-P_{xx})^{1/2}/\eta \tag{14}$$

The case of a separation with varying vorticity may also be considered but requires the inclusion of higher-order terms in Eq. (13). The general shape of the trajectories for such a case is shown in Fig. 7. At the critical point

$$P_{xx} = P_{zz} < 0, \qquad P_{yy} = 0$$

If at the critical point η is finite, then the trajectories in the immediate vicinity of the critical point must follow the degenerate pattern of case (1) above. Away from the critical point, the trajectories behave as though the critical point was "saddlelike," which is deduced from the expression for $\dot{y}/\dot{x}$ with higher-order terms included.

For this case, the separation angle is given by

$$\tan\theta = \pm 2(-P_{xx})^{1/2}/\eta_0 \tag{15}$$

where η_0 is the value of η at the critical point.

It should be noted that unlike the laminar flow case [Eq. (11)] the effect of three-dimensionality does not affect the functional form of Eq. (14) since the inclusion of higher-order terms causes no modification to the lower-order terms. Associated with three-dimensionality is varying vorticity and one must use η_0, the vorticity at the critical point, rather than an overall constant value of η as in two-dimensional flow.

A nominally two-dimensional separation bubble was set up by the authors to investigate the properties of near two-dimensional separation and reattachment. By measuring the separation and reattachment angles of the experimental streamline pattern and using the observed constant vorticity applicable to the bulk of the flow, the surface pressure variation could be predicted from Eq. (14), thus

$$P = P_0 - \frac{\eta^2 \tan^2\theta}{8} x^2 + \cdots \tag{16}$$

where P_0 is the pressure at the critical points. The resulting osculating parabolas are compared with experimental data in Fig. 8. This shows that the predicted scales are reasonable, and that such critical points are indeed points of maximum pressure.

In contrast, a critical point corresponding to case (3) is a pressure minimum and would be located at the centre of a separation bubble on a plane of symmetry. If the flow is three-dimensional, then far from such a critical point, the trajectories would spiral in (or out) and this requires higher-order terms in Eq. (13) since the vorticity would be varying. However, as the

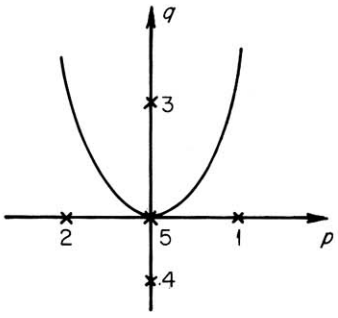
q
3
2
5
1
p
4

(a)

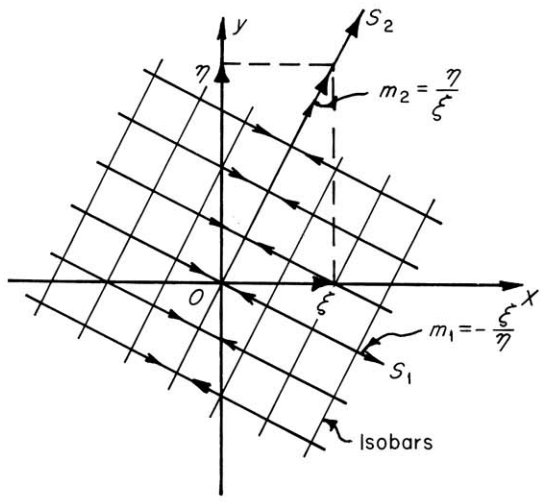
y
S_2
η
$m_2 = \frac{\eta}{\xi}$
O
ξ
X
$m_1 = -\frac{\xi}{\eta}$
S_1
Isobars

(b)

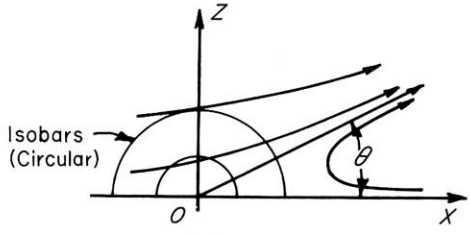
Z
Isobars
(Circular)
θ
O
X

(c)

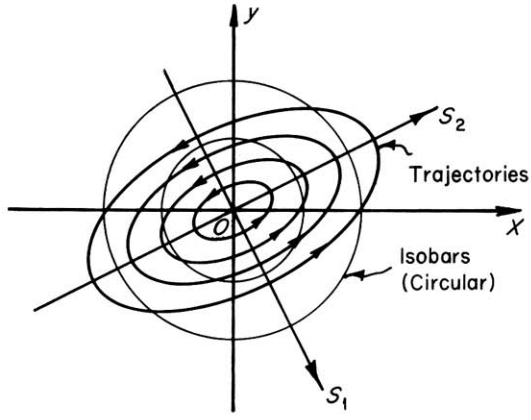
y
S_2
Trajectories
O
X
Isobars
(Circular)
S_1

(d)

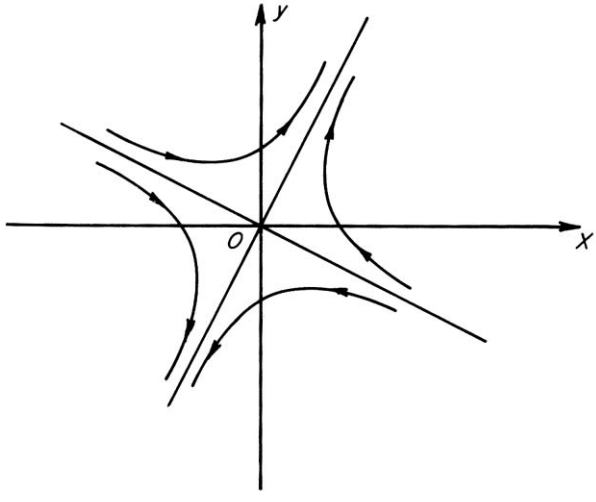

(e)

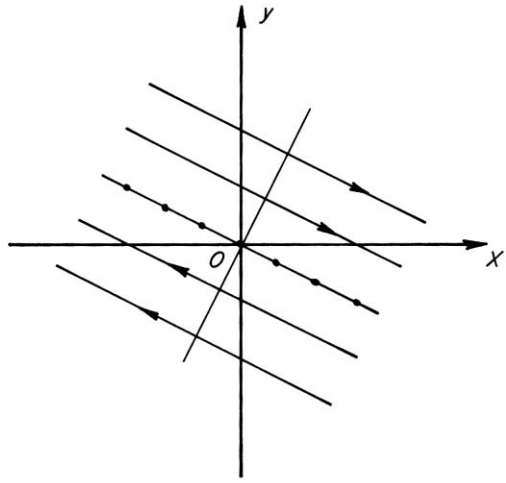

(f)

FIG. 6. Inviscid critical points. (a) p-q chart showing degenerate cases. (b) Cases 1 and 2. Degenerate node. Case 1 shown and case 2 has arrows reversed. P_{xx} and P_{yy} are finite. Maximum magnitude of second derivative of pressure is $|P_{s_1s_1}| = |P_{zz}|$. $P_{s_1s_1} < 0$ hence S_2 is a line of maximum pressure. $P_{s_2s_2} = 0$; $\zeta = 0$. S_1 and S_2 are orthogonal. (c) x-z plane trajectories for case 1 if S_2 and S_1 are rotated to y and x axes respectively. $P_{xx} = P_{zz} < 0$. (d) Case 3. Degenerate focus (or centre) $P_{xx} = P_{yy} > 0$. Critical point corresponds to a pressure minimum. $\xi = \eta = 0$. ζ is finite; $P_{zz} = 0$. Characteristic direction S_2 depends on one undetermined coefficient. Ratio of major to minor axes of ellipses depends on $P_{xx}^{1/2}/\zeta$. $\lambda_{1,2} = \pm j\omega$ where $j = (-1)^{1/2}$ and $\omega = P_{xx}^{1/2}$. For special cases of circular trajectories $\omega = \zeta/2$. (e) Case 4. Saddle. $P_{xx} = P_{yy} < 0$; $\xi = \eta = 0$, ζ is finite, $P_{xx} = 0$. Case similar to Fig. 6c. (f) Case 5. η, ξ, and ζ are finite; $P_{xx} = P_{yy} = P_{zz} = 0$.

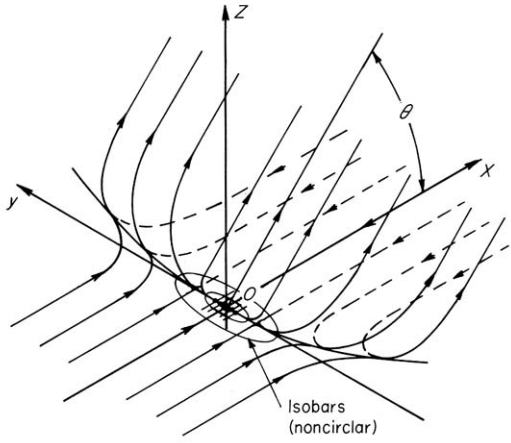

FIG. 7. Inviscid three-dimensional separation close to 0 $P_{xx} < 0$; $P_{yy} = 0$; $P_{zz} = P_{xx}$. If $\eta = \eta_0$ at 0 and is finite, trajectories follow degenerate pattern (Case 1, Fig. 6b) at 0.

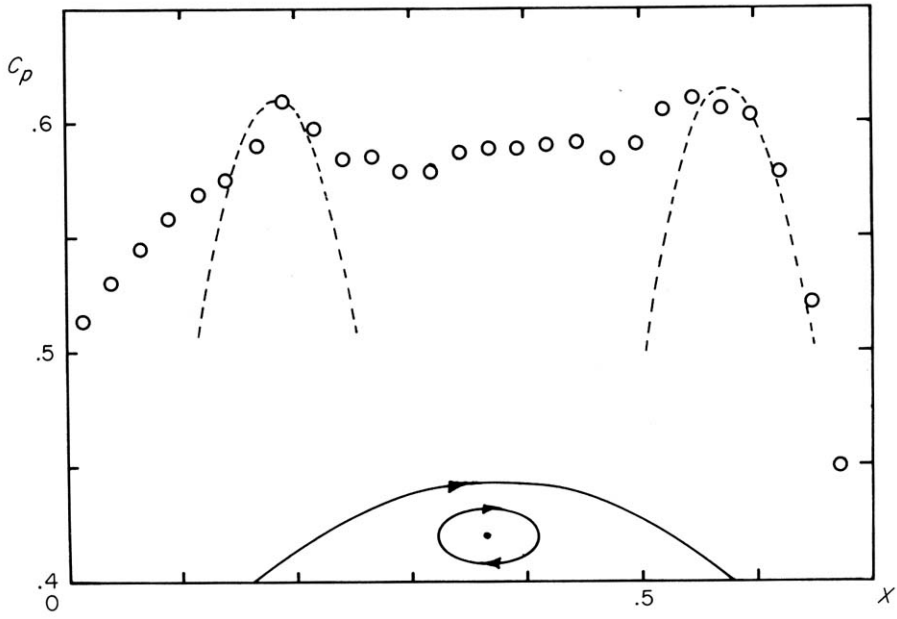

FIG. 8. Experimental near-two-dimensional separation bubble. Surface pressure measurements are compared with osculating parabolae given by Eq. (16). C_p is pressure coefficient and x is in meters.

critical point is approached, the linearised form (13) would be applicable giving a degenerate centre of constant vorticity. Thus trajectories would spiral in (or out) at an ever decreasing rate as the critical point is approached giving a "blob" of vorticity. Such blobs have been observed in smoke pattern studies.

An inviscid constant vorticity analysis is also applicable to laminar "viscous" flow provided the critical points under discussion occur away from the surface and provided the vorticity gradients at the points are

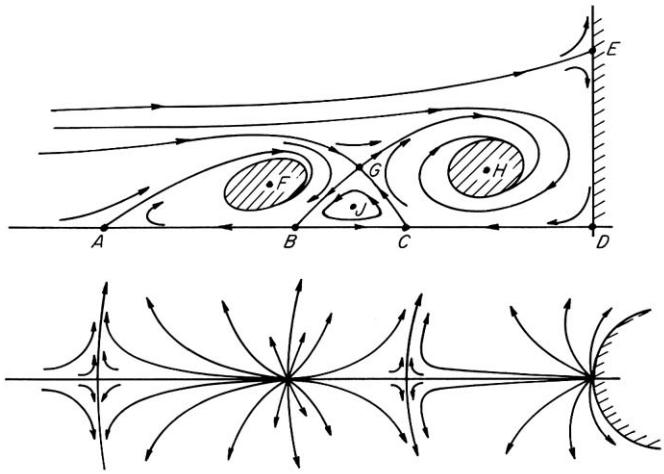

FIG. 9. Laminar separation in front of cylindrical obstruction. *A*, *B*, *C*, *D*, and *E* are viscous critical points. *F*, *G*, *H*, and *J* are inviscid-constant-vorticity critical points. Plan view shows surface trajectories. Note the sequence of saddles and nodes.

small. Figure 9 shows such critical points for the case of three-dimensional laminar flow separation upstream of a cylindrical obstruction (see Thwaites, 1960). Note the inviscid, constant-vorticity saddle-type critical point which occurs in "mid-air."

Figure 10 shows the conjectured (and partially verified) flow pattern which occurs when a turbulent boundary layer separates in front of a building with a causeway beneath. Critical points on salient edges such as appear in Fig. 10 can be treated using the analysis included here. Each flow approaching the edge in a plane of symmetry normal to the edge produces a saddle. The two saddles must be matched for pressure and velocity along their common sepratrix emanating from the edge. Assuming that the boundary layer flows approaching the edge are of constant but differing vorticity with slip, then as the vorticity ratio approaches infinity, the sepratrix streamline will leave the edge tangentially as shown in Fig. 10. The second derivative of pressure at the edge then goes to zero and this is consistent with free-streamline theory.

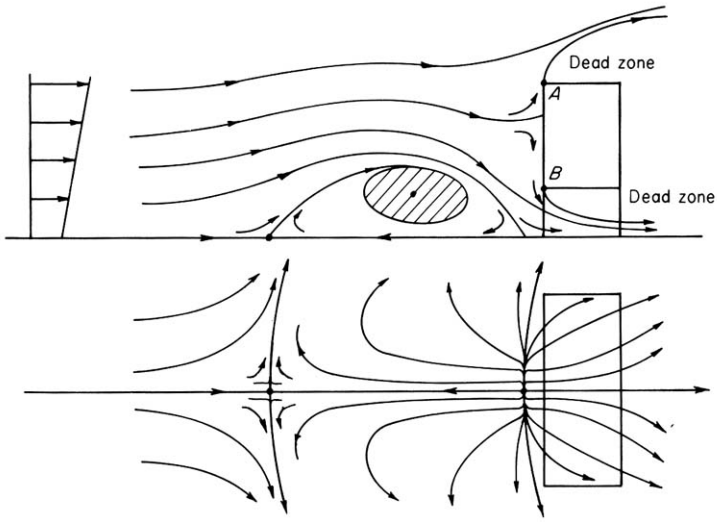

FIG. 10. Conjectured pattern for the separation of a turbulent boundary layer in front of a building with a causeway beneath. Plan view shows trajectories at ground level. *A* and *B* are salient edges.

5. Discussion and Conclusions

In the case of laminar separation and reattachment, the first derivative of pressure is finite and the vorticity is zero at the critical point. Contrary to this, turbulent boundary layer separation produces a critical point with zero first derivative of pressure and finite vorticity. This is simply a reflexion of the models being used. In the former, one has a balance of viscous and pressure gradient forces, while in the latter there is a balance of inertia and pressure gradient forces. Of course, in reality, a turbulent boundary layer has a viscous zone very close to the boundary where the no-slip condition applies. Hence the surface trajectories discussed for this case are really those which would exist if one extrapolated the outer rotational inviscid flow to the boundary. The thin, and hopefully unimportant viscous zone would have its own viscous critical points and so produce patterns which would need to match these outer patterns somewhere above the surface.

The description of flow patterns in terms of linearizable critical points as put forward by Lighthill and adopted here may not be without controversy. Maskell (1955) and recently Buckmaster (1972)[2] regard a separation line as an "envelope" to which other trajectories join tangentially. Indeed at first

[2] This work was brought to the authors' attention by Dr. J. Hunt of Cambridge, U.K. during the conference discussion.

sight, experiment would seem to support this viewpoint. However, to support this view theoretically, it would be necessary to show that a separation line was a singular solution to the Navier–Stokes equation. There is as yet no theoretical evidence to suggest that a curved singular solution is possible. The viewpoint adopted here leads to the suggestion that a separation line is a sepratrix to which the trajectories asymptote. Support for this view is convincing from an examination of the cases given in Fig. 3. If the index to the power law is small or large, calculations show that the trajectories asymptote to the sepratrix so rapidly that one could regard (or mistake) them as joining the sepratrix tangentially.

REFERENCES

Andronov, A. A., Vitt, A. A., and Khaikin, S. E. (1966). "Theory of Oscillators." Addison-Wesley, Reading, Massachusetts and Pergamon, Oxford.

Buckmaster, J. (1972). Perturbation technique for the study of three-dimensional separation. *Phys. Fluids* **15**, 2106–2113.

Fairlie, B. D. (1973). A study of separation in turbulent boundary layers. Ph.D. Thesis, Univ. of Melbourne, Melbourne.

Kaplan, W. (1958). "Ordinary Differential Equations." Addison-Wesley, Reading, Massachusetts and Pergamon, Oxford.

Kronauer, R. E. (1967). *In* "Fluid Mechanics of Internal Flow" (G. Sovran, ed.), p. 331. Elsevier, Amsterdam.

Lighthill, M. J. (1963). *In* "Laminar Boundary Layers" (L. Rosenhead, ed.), pp. 48–88. Oxford Univ. Press (Clarendon), London and New York.

Maskell, E. C. (1955). Flow separation in three dimensions. *R.A.E. Rep.* **Aero 2565**.

Oswatitsch, K. (1958). *In* "Die Ablönsungsbedingung von Grenzschichten, Grenzschicht Forschung" (H. Goertler, ed.), p. 357. Springer-Verlag, Berlin and New York.

Pontryagin, L. S. (1962). "Ordinary Differential Equations." Addison-Wesley, Reading, Massachusetts and Pergamon, Oxford.

Smith, P. D. (1970). A note on the computation of the inviscid rotational flow past the trailing edge of an aerofoil. *R.A.E. Tech. Memo.* **Aero 1217**.

Thwaites, B. (1960). "Incompressible Aerodynamics," First Plate. Oxford Univ. Press (Clarendon), London and New York.